Damping torque analysis for DC bus implemented damping control

Published in:
European Transactions on Electrical Power

Queen's University Belfast - Research Portal:
[Link to publication record in Queen's University Belfast Research Portal](#)

Damping Torque Analysis for DC Bus Implemented Damping Control

Abstract – Damping torque analysis is a well-developed technique for understanding and studying power system oscillations. This paper presents the applications of damping torque analysis for DC bus implemented damping control in power transmission networks in two examples. The first example is the investigation of damping effect of shunt voltage source converter (VSC) based flexible AC transmission systems (FACTS) voltage control, i.e. static synchronous compensator (STATCOM) voltage control. It is shown in the paper that STATCOM voltage control mainly contributes synchronous torque and hence has little effect on the damping of power system oscillations. The second example is the damping control implemented by a battery energy storage system (BESS) installed in a power system. Damping torque analysis reveals that when BESS damping control is realized by regulating exchange of active and reactive power between the BESS and power system, respectively, BESS damping control exhibits different properties. It is concluded by damping torque analysis that BESS damping control implemented by regulating active power is better with less interaction with BESS voltage control and more robust to variations of power system operating conditions. In the paper, all analytical conclusions obtained are demonstrated by simulation results of example power systems.

1. INTRODUCTION

Since it was proposed, damping torque analysis has been widely used in the engineering practice in power system damping control to suppress low-frequency oscillations and improve power system stability [1]. Damping torque analysis is established on the Phillips-Heffron model of single-machine infinite-bus power systems [2] and based on the concept of damping torque contribution to the rotor motion of synchronous generators and classical control theory. It was firstly proposed to study the damping affect of excitation control systems [3]. Later it was used to design Power System Stabilizer (PSS) [4] via the phase compensation method, a milestone indicating the full benefit of damping torque analysis applied in power system control. With clear physical background and engineering insight provided, damping torque analysis has been one of the most successful engineering techniques proposed so far in the field of power system control for the analysis and design of damping control systems implemented via excitation of synchronous generator, such as PSS.

More recently, damping torque analysis has been used to investigate the damping effect of a newly appeared technology of Flexible AC Transmission Systems (FACTS) [5]. Detailed theoretical analysis by using the damping torque analysis is presented in [6][7] for the conventional thyristor-based FACTS devices such as SVC (Static Var Compensator) and TCSC (Thyristor Controlled Series Compensator). Many useful conclusions have been

obtained that provide valuable guidelines for and insight into the FACTS applications to suppress power system oscillations. For example, one of them is about the SVC voltage control imposing no effect on the damping of power system oscillations. It is proved in [6] by using the damping torque analysis that SVC voltage control provides no damping torque. This analytical conclusion has confirmed previous findings from calculation and simulation of practical examples. However, when the damping torque analysis is applied to the new generation of VSC based FACTS devices, such as STATCOM (Static Synchronous Compensator)and UPFC (Unified Power Flow Controller), it has been found that the analysis becomes extremely difficult [8][9]. That is because the integration of DC bus of VSC FACTS devices has led to complicated mathematical expressions of damping torque contributions from VSC FACTS devices. No analytical conclusions can be drawn by simply observing those mathematical expressions instead of numerical calculation.

With the recent active research and development in renewable generation, Energy Storage System (ESS) is being considered to be applied in power transmission systems to accommodate the intermittence of renewable generation. Commonly used ESS can be battery ESS, flywheel ESS, Supercapacitor and Superconducting Magnetic Energy Storage (SMES). It is expected that ESS will significantly assist the operation and control of power systems, including the improvement of power system stability [10]. In fact, theoretical research and laboratory experiment have demonstrated that SMES, as one of typical ESS applied in power systems, can effectively suppress power system oscillations [11]. Field application has also shown that battery ESS can provide damping to power system oscillations and enhance system stability [12].

VSC based FACTS devices and ESS are set up on DC bus and connected to power transmission network via an interface of inverter. Damping control is superimposed on the normal control function implemented through regulating the modulation ratio and phase of the inverter, leading to exchange of active and reactive power of FACTS and ESS with the rest of a power system. Hence in this paper, damping torque analysis will be carried out for VSC based FACTS devices and ESS, which is represented by a DC bus in the AC transmission network. This representation significantly simplifies the damping torque analysis and makes theoretical analysis possible, as to be demonstrated by two practical examples in the paper. The first example is the analysis of damping effect of STATCOM voltage control. It is proved in the paper that STATCOM voltage control only contributes synchronous torque and hence imposes no effect on the damping of power system oscillations. The second example is the investigation of damping control implemented by battery Energy Storage Systems (ESS). It is established in the paper that both the interaction between battery ESS damping and voltage control and the robustness of battery ESS damping control to the variations of power flow conditions is different when it is implemented via battery ESS active and reactive power regulation respectively. In the paper, all conclusions are demonstrated by simulation results of example power systems installed with a STATCOM and a battery ESS separately.

2. POWER SYSTEM EMBEDDED WITH DC BUS

A single-machine infinite-bus power system is shown by Figure 1, where a shunt-connected

DC bus is at busbar s. $\overline{V}_C$ at the AC terminal of the inverter (VSC) is regulated by

modulation ratio m and phase γ respectively. Hence at the power system level, regulation of

magnitude and phase of $\overline{V}_C$ determines the exchange of reactive and active power between

the DC bus and the power system respectively.
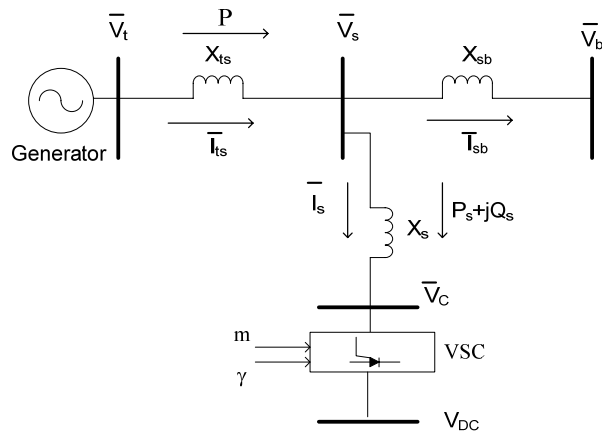
Figure 1 A power system with a shunt-connected DC bus

From Figure 1 it can be established that

$$\overline{V}_S = \frac{jX_{sb}}{1+\dfrac{X_{sb}}{X_S}}\overline{I}_{ts} + \frac{X_{sb}}{X_S(1+\dfrac{X_{sb}}{X_S})}\overline{V}_C + \frac{\overline{V}_b}{1+\dfrac{X_{sb}}{X_S}} \tag{1}$$

That gives

$$\overline{V}_t = jX_{ts}\overline{I}_{ts} + \overline{V}_S = j(X_{ts} + \frac{X_S X_{sb}}{X_S + X_{sb}})\overline{I}_{ts} + \frac{X_{sb}}{X_S + X_{sb}}\overline{V}_C + \frac{X_S}{X_S + X_{sb}}\overline{V}_b = jX\overline{I}_{ts} + \overline{V} \quad (2)$$

where

$$X = (X_{ts} + \frac{X_S X_{sb}}{X_S + X_{sb}}) \qquad \overline{V} = \frac{X_{sb}}{X_S + X_{sb}}\overline{V}_C + \frac{X_S}{X_S + X_{sb}}\overline{V}_b = a\overline{V}_C + b\overline{V}_b$$

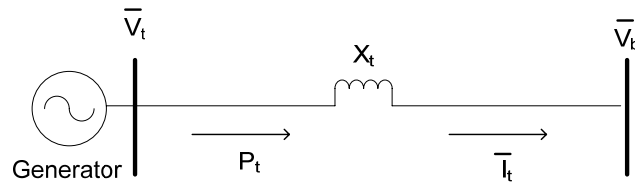For a single-machine infinite-bus power system without the DC bus as shown by Figure 2, voltage equation of the system is

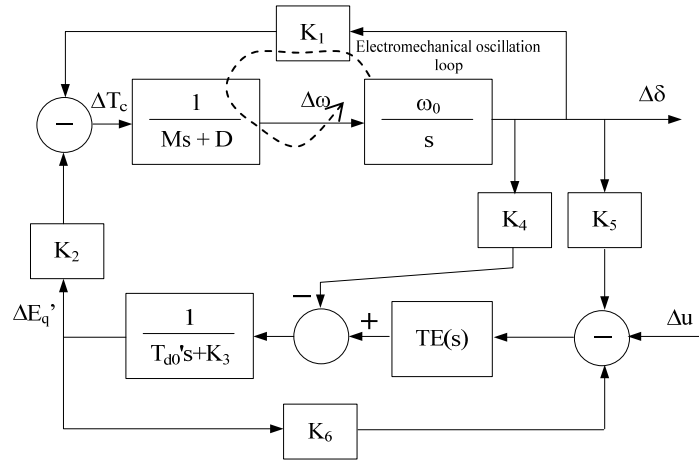$$\overline{V}_t = jX_t\overline{I}_t + \overline{V}_b \tag{3}$$

and active power supplied by the generator is

$$P_t = \frac{E_q'V_b}{x'_{d\Sigma}}\sin\delta - \frac{V_b^2}{2}\frac{(x_q - x_d')}{x'_{d\Sigma}\,x_{q\Sigma}}\sin 2\delta \tag{4}$$

where δ is the angle (load angle) between E_q' and V_b and $x'_{d\Sigma} = X_t + X_d'$, $x_{q\Sigma} = X_t + X_q$.

Figure 3 Phillips-Heffron model

Damping torque analysis of power system of Figure 2 is based on its linearized Phillips-Heffron model as shown by Figure 3, where the electric torque contributed into the electromechanical oscillation loop is ΔT_e. ΔT_e can be decomposed into synchronous torque $C_s\Delta\delta$ and damping torque $C_d\Delta\omega$ as follows

$$\Delta T_e = \Delta P_t = C_s\Delta\delta + C_d\Delta\omega \tag{5}$$

Contribution of damping torque $C_d\Delta\omega$ determines the damping of power system oscillations [1].

Comparing Eq.(2) and (3) it can be seen that the power system embedded with DC bus of

Figure 1 is electrically equivalent to the power system of Figure 2. Replacing X_t and V_b in

Eq.(4) by X and $\overline{V}$ respectively, it can be obtained that the active power delivered along the

transmission line in the power system of Figure 1 is

$$P = \frac{E_q'V}{x'_{d\Sigma}} \sin \delta' - \frac{V^2}{2} \frac{(x_q - x_d')}{x'_{d\Sigma} \, x_{q\Sigma}} \sin 2\delta' \tag{6}$$

where δ' is the angle between E_q' and $\overline{V}$ and $x'_{d\Sigma} = X + X_d'$, $x_{q\Sigma} = X + X_q$.
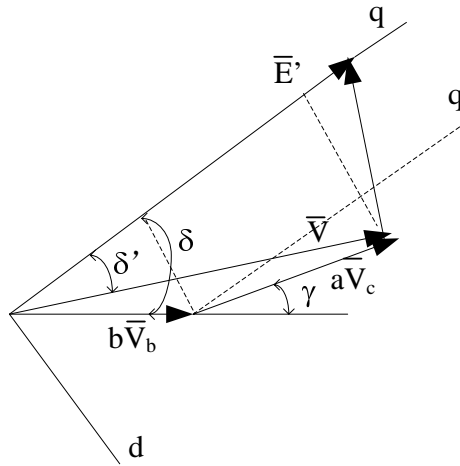
Figure 4 Phasor diagram

From phasor diagram of Figure 4 it can have

$$V \sin \delta' = bV_b \sin \delta + aV_c \sin(\delta - \gamma) \,; \; V \cos \delta' = bV_b \cos \delta + aV_c \cos(\delta - \gamma) \tag{7}$$

Hence from Eq.(6) and (7) it can obtained that

$$P = \frac{E_q{}'}{x'_{d\Sigma}}[bV_b \sin\delta + aV_c \sin(\delta - \gamma)]$$
$$-\frac{(x_q - x_d{}')}{x'_{d\Sigma} \, x_{q\Sigma}}[bV_b \sin\delta + aV_c \sin(\delta - \gamma)][bV_b \cos\delta + aV_c \cos(\delta - \gamma)]$$

(8)

3. EXAMPLE 1 – STATCOM VOLTAGE CONTROL

For the power system of Figure 1, when it is a STATCOM installed at busbar s, the DC voltage at the DC bus is supported by a capacitor C and [13]

$$V_c = mkV_{DC} \quad (k \text{ is a constant dependent of the structure of inverter}) \tag{9}$$

STATCOM voltage control is implemented by controlling the modulation ratio m. There is no exchange of active power between the STATCOM and power system and hence modulation phase γ is kept constant. For the simplicity of analysis, it is assumed that STATCOM voltage control adopts a proportional control law, that is

$$m = m_0 + K_V(V_{sref} - V_s) \tag{10}$$

From Eq.(5) it is known that the electric torque contributed by the STATCOM voltage

control is

$$\Delta T_{statcom} = \Delta P_{statcom} = \frac{\partial P}{\partial m}\Delta m = \frac{\partial P}{\partial V_c}\frac{\partial V_c}{\partial m}\Delta m \tag{11}$$

From Eq.(8) and (9) it can be obtained that

$$\frac{\partial P}{\partial V_c} = C_P = \frac{E_{q0}{}'}{x'_{d\Sigma}}a\sin(\delta_0 - \gamma_0) - \frac{(x_q - x_d{}')}{x'_{d\Sigma}\ x_{q\Sigma}}[bV_{b0}\sin\delta_0 + aV_{c0}\sin(\delta_0 - \gamma_0)]$$

$$a\cos(\delta_0 - \gamma_0) - \frac{(x_q - x_d{}')}{x'_{d\Sigma}\ x_{q\Sigma}}[bV_{b0}\cos\delta_0 + aV_{c0}\cos(\delta_0 - \gamma_0)]a\sin(\delta_0 - \gamma_0)$$

$$\frac{\partial V_c}{\partial m} = C_m = kV_{DC} \tag{12}$$

Linearization of Eq.(9) and (10) gives (PWM is used and hence V_{DC} is kept constant [13])

$$\Delta V_c = kV_{DC}\Delta m$$

$$\Delta m = -K_V\Delta V_s \tag{13}$$

Eq.(13) and (I3) in Appendix give

$$\Delta m = \frac{1}{kV_{DC}}\frac{-K_V kV_{DC}C_1}{1 + K_V kV_{DC}C_2}\Delta\delta \tag{14}$$

Hence from Eq.(11), (12) and (14) it can be obtained that the electric torque contributed by STATCOM voltage control is

$$\Delta T_{statcom} = C_P \frac{-K_V k V_{DC} C_1}{1 + K_V k V_{DC} C_2} \Delta \delta \tag{15}$$

From the point view of power system operation and control, voltage control implemented by SVC and STATCOM is same, though performance of STATCOM voltage control is better. In [14] and [15], from simulation results of practical examples, it was found that SVC voltage control has little influence on the damping of power system oscillations no matter how strong the voltage control is. This finding is proved mathematically in [16] by using damping torque analysis. In [7] the same phenomenon about the STATCOM voltage control imposing no effect on the damping of power system oscillations is reported from simulation results of practical examples. However, [7] does not provide a mathematical proof. Here from Eq.(5) and (15) it can be immediately concluded that STATCOM voltage control only provides synchronous torque and hence imposes no effect on the damping of power system oscillations. Thus the mathematical proof to the finding in [7] is provided.
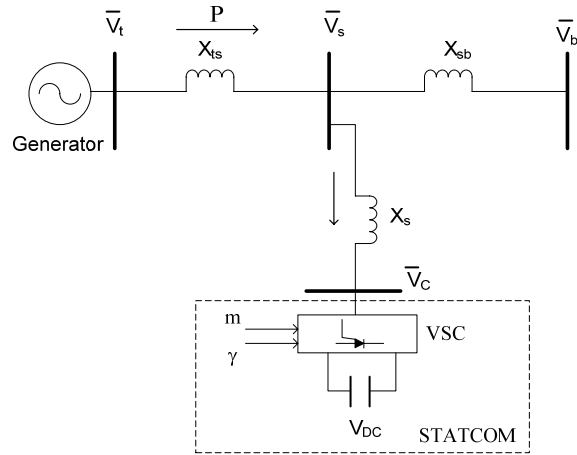
Figure 5 An example power system installed with a STATCOM

An example power system with a STATCOM installed is shown by Figure 5. System parameters and initial operating condition are

Transmission line: $X_{ts} = 0.3 p.u., X_{sb} = 0.3 p.u., X_s = 0.3 p.u.$;

Generator: $X_d = 0.8 p.u., X_q = 0.4 p.u., X'_d = 0.2 p.u., M = 8s., D = 0 p.u., T'_{d0} = 5s.$;

AVR: $T_A = 0.01s. K_A = 100 p.u.$; STATCOM: $C = 1.0 p.u., V_{DC} = 1.0 p.u.$

Initial load condition: $V_{t0} = 1.0 p.u., V_{s0} = 1.0 p.u., V_{b0} = 1.0 p.u., P_{ts0} = 0.5 p.u.$

Figure 6 shows the small-signal simulation results (1% increase of mechanical power input at 1.0 second of simulation for 100ms.) of the power system without STATCOM voltage control and with a PI voltage controller applied (with $K_{VP} = 0.1, K_{VI} = 10$). From Figure 6 it can be seen that STATCOM voltage control has little influence on the damping of power system oscillation as it is concluded from the above damping torque analysis. In the simulation presented in Figure 6, STATCOM voltage control adopts the realistic

proportional and integral control law and detailed non-linear model of example power system is used. Hence simulation results confirm not only the analytical results but also the simplification used in the damping torque analysis.
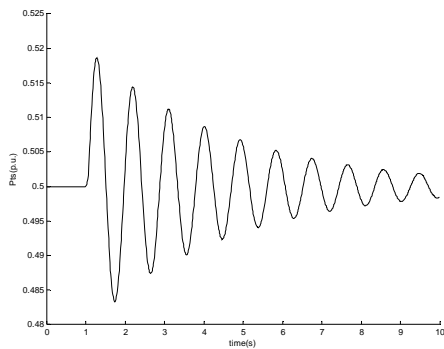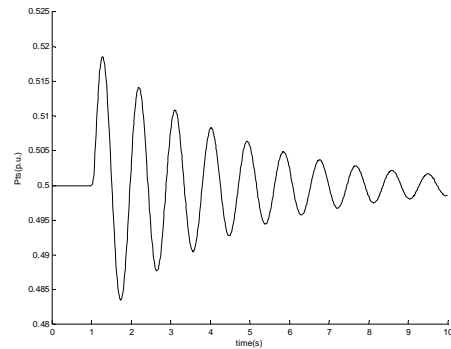

(a) without STATCOM voltage control   (b) with STATCOM voltage control

Figure 6 Simulation results of example power system of Figure 5

4. EXAMPLE 2 – BATTERY ENERGY STORAGE SYSTEM

A damping control function can be implemented by a battery ESS to improve damping of power system oscillations. Dynamic model of the battery ESS is shown by Figure 7 [13]. For the simplicity of analysis, the slow dynamics of function of active power and frequency regulation of battery ESS is ignored. It is assumed that the damping control adopts a proportional control law and the damping feedback signal is the rotor speed of the generator (If a locally available signal, such as the active power delivered along the transmission line, is used, it can always be represented as the linear combination of rotor angle and rotor speed. This will not change the discussion below). Damping control can be added on the

voltage control function of battery ESS or implemented by controlling VSC modulation phase γ directly as shown in Figure 7.
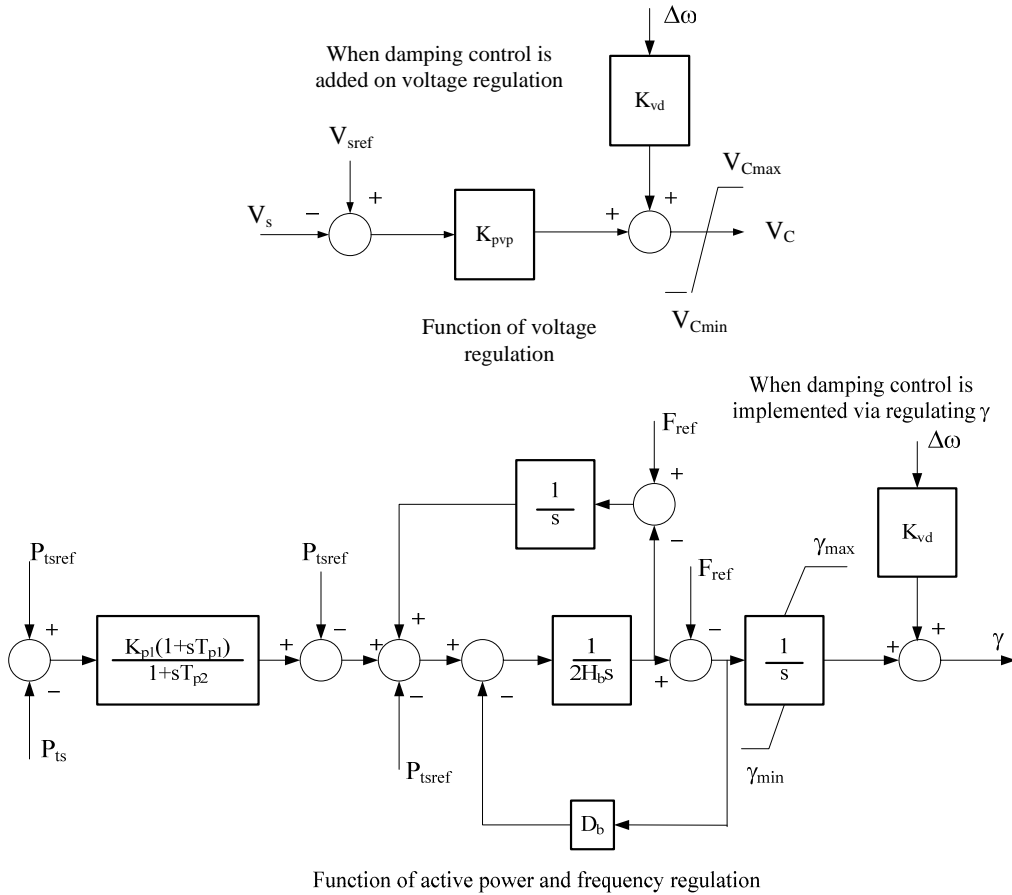
Figure 7 Dynamic model of battery ESS

For the first case when damping control is added on voltage regulation,

$$V_c = V_{c0} + K_{pvp}(V_{sref} - V_s) + K_{vd}\Delta\omega \tag{16}$$

Linearization of above equation gives

$$\Delta V_c = -K_{pvp} \Delta V_s + K_{vd} \Delta \omega \tag{17}$$

Eq.(17) and (I3) in Appendix give

$$\Delta V_c = \frac{-K_{pvp} C_1}{1 + K_{pvp} C_2} \Delta \delta - \frac{K_{vd}}{1 + K_{pvp} C_2} \Delta \omega \tag{18}$$

In Eq.(8)

$$P = \frac{E_q{}'}{x'_{d\Sigma}} [bV_b \sin\delta + aV_c \sin(\delta - \gamma)] >>$$

$$\frac{(x_q - x_d{}')}{x'_{d\Sigma} x_{q\Sigma}} [bV_b \sin\delta + aV_c \sin(\delta - \gamma)][bV_b \cos\delta + aV_c \cos(\delta - \gamma)]$$

Hence

$$P \approx \frac{E_q{}'}{x'_{d\Sigma}} [bV_b \sin\delta + aV_c \sin(\delta - \gamma)] \tag{19}$$

From Eq.(18) and (19) it can be obtained that

$$\Delta T_{ESS} = \Delta P_{ESS} = \frac{\partial P}{\partial V_C} \Delta V_C = \frac{E_{q0}{}'}{x'_{d\Sigma}} a \sin(\delta_0 - \gamma_0)(\frac{-K_{pvp} C_1}{1 + K_{pvp} C_2} \Delta \delta - \frac{K_{vd}}{1 + K_{pvp} C_2}) \Delta \omega$$

Hence according to Eq.(5), damping torque contributed from the damping control of battery ESS is

$$\Delta T_{ESSD} = -\frac{E_{q0}{}'}{x'_{d\Sigma}} a \sin(\delta_0 - \gamma_0)\frac{K_{vd}}{1 + K_{pvp}C_2}\Delta\omega \qquad (20)$$

For the second case when damping control is implemented via regulating γ,

$$V_c = V_{c0} + K_{pvp}(V_{sref} - V_s); \quad \gamma = \gamma_0 + K_{vd}\Delta\omega \qquad (21)$$

Linearization of above equation gives

$$\Delta V_c = -K_{pvp}\Delta V_s; \quad \Delta\gamma = K_{vd}\Delta\omega \qquad (22)$$

Eq.(22) and Eq.(I3) in Appendix give

$$\Delta V_c = \frac{-K_{pvp}C_1}{1 + K_{pvp}C_2}\Delta\delta - \frac{K_{pvp}C_3}{1 + K_{pvp}C_2}K_{vd}\Delta\omega \qquad (23)$$

In this case, electric torque contributed by damping control is

$$\Delta T_{ESS} = \Delta P_{ESS} = \frac{\partial P}{\partial V_C}\Delta V_C + \frac{\partial P}{\partial\gamma}\Delta\gamma \qquad (24)$$

and from Eq.(5), (19), (23) and (24) the damping torque contributed by the damping control of battery ESS in this case can be obtained to be

$$\varDelta T_{ESSD} = \frac{E'_0}{X'_\Sigma} aV_{c0}K_{vd}[\sin(\delta_0 - \gamma_0)\frac{K_{pvp}C_3}{1 + K_{pvp}C_2} + \cos(\delta_0 - \gamma_0)] \tag{25}$$

By observing Eq.(20) and (25), it can be concluded that damping torque contribution from the damping control of battery ESS is different when it is implemented differently in the following two aspects

(1) When the voltage control is strengthened with a higher gain value, K_{pvp}, damping torque contribution decreases more when damping control is added on the function of voltage control than when it is implemented via regulating γ. This means there is stronger interaction between the voltage and damping control of battery ESS when damping control is added on the function of voltage control;

(2) With the variation of load condition, i.e., $(\delta_0 - \gamma_0)$, damping torque contribution changes more when damping control is added on the voltage control function than when it is implemented via regulating γ.

Two conclusions of damping torque analysis above can be further demonstrated by simulation results of an example power system with the same configuration of Figure 5, where STATCOM is replaced by a battery ESS. Figure 8 shows the simulation results when

damping control is added on the function of voltage control of the battery ESS with different value of gain of voltage control. From Figure 8 it can be clearly seen that with the increase of voltage control strength, effectiveness of damping control of battery ESS decreases. However, when damping control is implemented directly by regulating γ, there is no such interaction between voltage and damping control of battery ESS, as shown by the simulation results presented in Figure 9. This confirms conclusion (1) above.

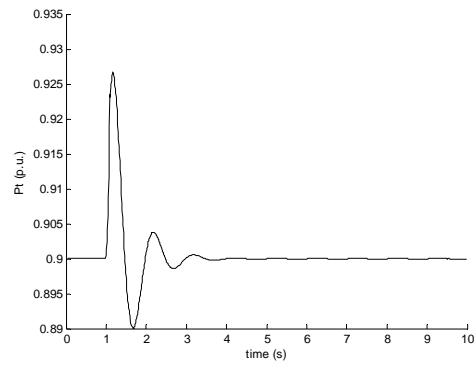$$K_{pvp} = 1 \qquad\qquad K_{pvp} = 3$$
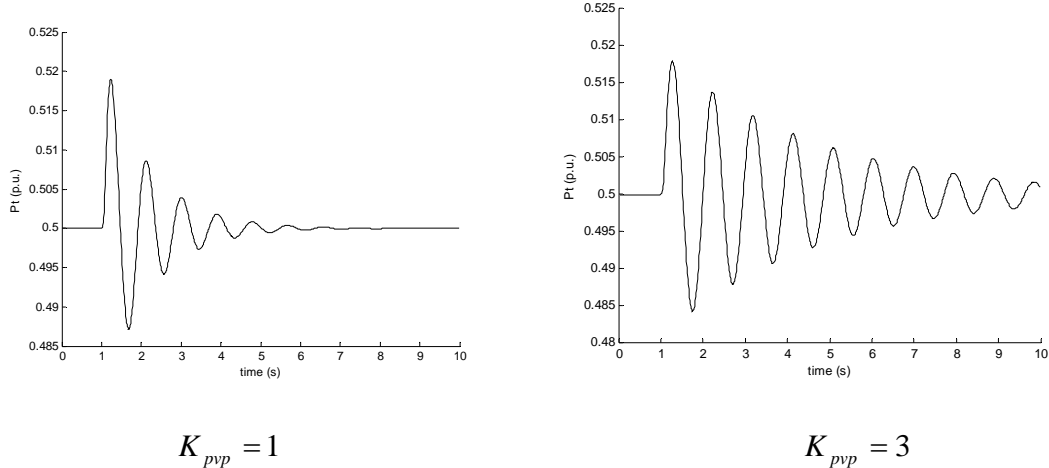
Figure 8 Simulation results with damping control superimposed on voltage control

$$K_{pvp} = 20 \qquad\qquad K_{pvp} = 300$$
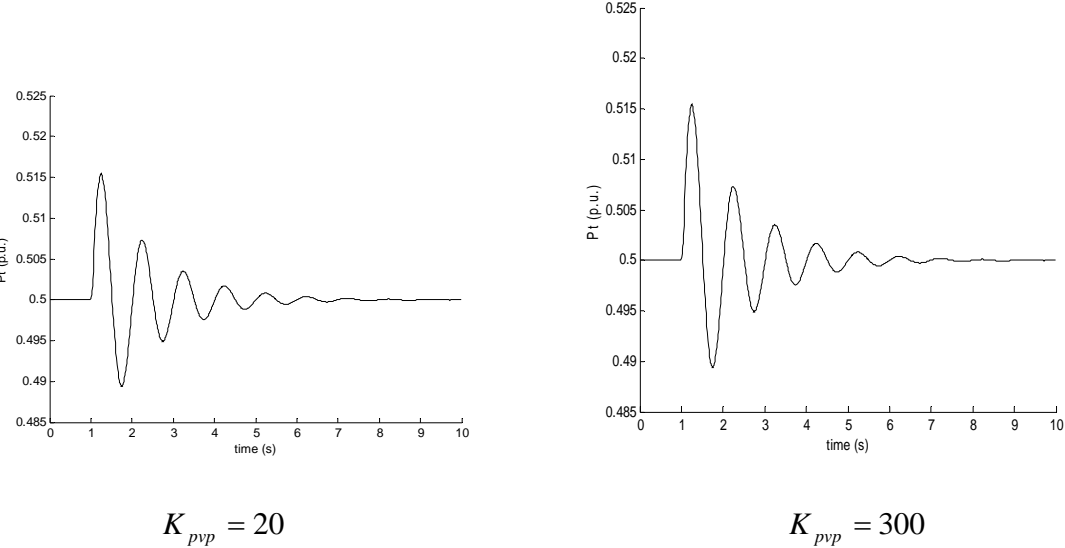
Figure 9 Simulation results with damping control implemented by regulating γ
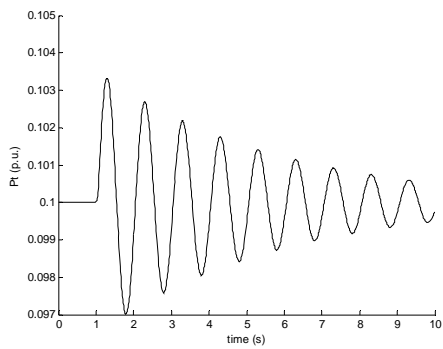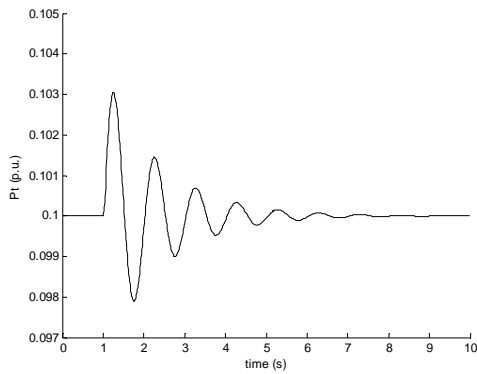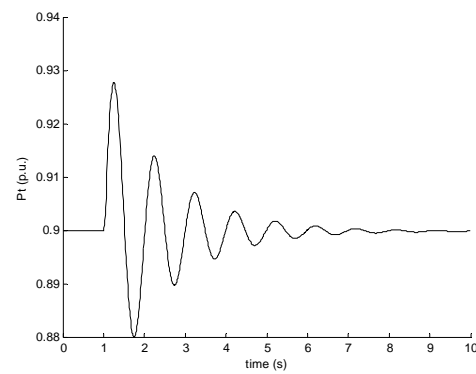
$$P_{ts} = 0.1 p.u.$$ $$P_{ts} = 0.9 p.u.$$

Figure 10 Simulation results with damping control superimposed on the voltage control

$$P_{ts} = 0.1 p.u.$$ $$P_{ts} = 0.9 p.u.$$

Figure 11 Simulation results with damping control implemented by regulating γ

To see the variation of effectiveness of damping control with changes of system load conditions, Figure 10 and 11 gives simulation results when damping control is added on voltage control and implemented directly by regulating γ respectively at two different load conditions, $P_{ts} = 0.1$p.u. and $P_{ts} = 0.9$p.u. From Figure 10 it can be seen that at a lower load condition, damping control is less effective when it is added on voltage control. However, from Figure 11 it can be seen that the effectiveness of damping control changes very little

when it is implemented by regulating γ. This means that the robustness of damping control is better if it is implemented by regulating γ.

Power system oscillations are variations of active power delivered along the transmission line. When damping control is added on the voltage control function of battery ESS, damping effect is achieved by regulating V_C, resulting in the exchange of reactive power between the battery ESS and the rest of power system. This exchange of reactive power affects the flow of active power along the transmission line and ultimately functions to suppress the power oscillations. Hence the effectiveness of the damping control in this case is influenced by the capability of voltage control to regulate the exchange of reactive power between the battery ESS and power system, i.e., the strength of voltage control. Furthermore, it is determined by the extent of influence of exchange of reactive power on the variations of active power delivered along the transmission line, which is affected by system load conditions. However, when the damping control is implemented directly by regulating γ, it results in the exchange of active power between the battery ESS and the rest of power system. Damping control functions for the battery ESS to absorb or release active power with the variations of active power delivered along the transmission line. The capability of absorbing or releasing active power is only determined by damping control and is not affected by its voltage control and relationship between active and reactive power flow at all. Hence this is the case that no interaction between the voltage and damping control of battery ESS can be observed and effectiveness of damping control changes little with variations of system load conditions.

5. CONCLUSIONS

Major contributions of this paper are the applications of damping torque analysis to the damping control function implemented by regulating DC bus embedded in power transmission networks. Detailed analysis is carried out in two practical examples, STATCOM voltage control and battery ESS damping control. Damping torque analysis has led to the following conclusions

(1) STATCOM voltage control only provides synchronizing torque to power systems and hence does not affect the damping of power system oscillations.

(2) When battery ESS damping control is superimposed on its voltage control function, it interacts with the normal voltage control and its effectiveness varies with the changes of system load conditions. However, when damping control is implemented by regulating γ, resulting direct exchange of active power between the battery ESS and the rest of power system, it does not interact with voltage control and is of better robustness to the variations of system load conditions.

All the conclusions obtained in the paper are demonstrated by simulation results of example power systems.

6. REFERENCES

[1] Y. N. Yu, Electric Power System Dynamics, Academic Press Inc., 1983

[2] W.G.Heffron and R.A.Phillips, "Effect of a modem amplidyne voltage regulator on under excited operation of large turbine generator", AIEE Trans. 71, 1952

[3] F.P.de Mello and C.Concordia, "Concept of Synchronous Machine Stability as Affected by Excitation Control", IEEE Tran. on PAS, Vol. 88, No. 4, April 1969, pp316-329

[4] E.V.Larsen and D.A.Swann, "Applying Power System Stabilizer, Part I-III", IEEE Trans. on PAS, Vol. 6, June 1981, pp3034-3046

[5] Y.H.Song and A.J.Johns, Flexible A.C. Transmission Systems, IEE Power, 1999

[6] H.F.Wang and F.J.Swift, 'The capability of the Static Var Compensator in damping power system oscillations', IEE Proc. Part C, May, No.4, 1996

[7] F.J.Swift and H.F.Wang, 'Application of the Controllable Series Compensator in damping power system oscillations', IEE Proc. Part C, May, No.4, 1996

[8] H.F.Wang, 'Phillips-Heffron model of power systems installed with STATCOM and applications', IEE Proc. Part C. No.5, 1999

[9] H.F.Wang, 'Damping function of Unified Power Flow Controller' IEE Proc. Part C, No.1, 1999

[10] Ribeiro P F, Johnson B K, Crow M L, Arsoy A and Liu Y, "Energy Storage Systems for advanced power applications", IEEE Proc., Vol. 89, No. 12, Ｄec.2001

[11] Hsu, C.-S.; Lee, W.-J., "Superconducting magnetic energy storage for power system applications", IEEE Trans. on Industry Applications, Vol.29, No.5, Sept.-Oct. 1993

[12] Bhargava, B.; Dishaw, G., "Application of an energy source power system stabilizer on the 10 MW battery energy storage system at Chino substation", IEEE Trans. on Power Systems, Vol.13, No.1, Feb. 1998

[13] CIGRE report TF38-01-08 "Modeling of power electronics equipment (FACTS) in load flow and stability programs", 1999

[14] Hammad, A.E., "Analysis of power system stability enhancement by static Var compensator", IEEE Trans, 1986, PWRS-1 (4)

[15] Zhou, E.Z., "Application of static Var compensators to increase power system damping", IEEE Trans., 1993, PWRS-8 (2)

[16] H.F.Wang and F.J.Swift, 'The capability of the Static Var Compensator in damping power system oscillations', IEE Proc. Part C, May, No.4, 1996

ACKNOWLEDGEMENTS

APPENDIX

For the power system of Figure 2 we have [1]

$$I_{tq} = \frac{V_b \sin\delta}{X_{q\Sigma}}; \qquad I_{td} = \frac{E_q{}' - V_b \cos\delta}{X_{d\Sigma}{}'}; \qquad x'_{d\Sigma} = X_t + X_d{}', x_{q\Sigma} = X_t + X_q \qquad \text{(I1)}$$

Replacing X_t and V_b in Eq.(I1) by X and $\overline{V}$ respectively, the following can be obtained for the power system with embedded DC bus

$$I_{tsq} = \frac{bV_b \sin\delta + aV_c \sin(\delta-\gamma)}{X_{q\Sigma}}, I_{tsd} = \frac{E_q{}' - bV_b \cos\delta - aV_c \cos(\delta-\gamma)}{X_{d\Sigma}{}'} \qquad \text{(I2)}$$

$$x'_{d\Sigma} = X + X_d{}', x_{q\Sigma} = X + X_q$$

From Figure 2 it can be established that $\overline{V}_t = jX_{ts}\overline{I}_{ts} + \overline{V}_s$. Hence Eq.(I2) gives

$$V_{sd} = (X_q + X_{ts})I_{tsq} = \frac{X_{ts\Sigma}}{X_{q\Sigma}}[bV_b \sin\delta + aV_c \sin(\delta-\gamma)]$$

$$V_{sq} = E_q{}' - (X_{ts} + X_d{}')I_{tsd} = E_q{}' - \frac{X_{ts\Sigma}{}'}{X_{d\Sigma}{}'}(E_q{}' - V\cos\delta')$$

$$= \frac{X_{d\Sigma}{}' - X_{ts\Sigma}{}'}{X_{d\Sigma}{}'}E_q{}' + \frac{X_{ts\Sigma}{}'}{X_{d\Sigma}{}'}[bV_b \cos\delta + aV_c \cos(\delta-\gamma)]$$

That gives

$$\Delta V_{sd} = \frac{X_{ts\Sigma}}{X_{q\Sigma}}[bV_{b0}\cos\delta_0 + aV_{c0}\cos(\delta_0 - \gamma_0)]\Delta\delta$$

$$+ \frac{X_{ts\Sigma}}{X_{q\Sigma}}aV_{c0}\sin(\delta_0 - \gamma_0)\Delta V_c - \frac{X_{ts\Sigma}}{X_{q\Sigma}}aV_{c0}\cos(\delta_0 - \gamma_0)\Delta\gamma$$

$$\Delta V_{sq} = -\frac{X_{ts\Sigma}}{X_{d\Sigma}'}[bV_{b0}\sin\delta_0 + aV_{c0}\sin(\delta_0 - \gamma_0)]\Delta\delta$$

$$+ \frac{X_{ts\Sigma}}{X_{d\Sigma}'}aV_{c0}\cos(\delta_0 - \gamma_0)\Delta V_c + \frac{X'_{ts\Sigma}}{X'_{\Sigma}}aV_{c0}\sin(\delta_0 - \gamma_0)\Delta\gamma$$

Hence

$$\Delta V_s = \frac{1}{V_{s0}}(V_{sd0}\Delta V_{sd} + V_{sq0}\Delta V_{sq}) = C_1\Delta\delta + C_2\Delta V_c + C_3\Delta\gamma \qquad (\text{I3})$$

where

$$C_1 = \frac{V_{sd0}X_{ts\Sigma}}{V_{s0}X_{q\Sigma}}[bV_{b0}\cos\delta_0 + aV_{c0}\cos(\delta_0 - \gamma_0)] - \frac{V_{sq0}X_{ts\Sigma}}{V_{s0}X_{d\Sigma}'}[bV_{b0}\sin\delta_0 + aV_{c0}\sin(\delta_0 - \gamma_0)]$$

$$C_2 = \frac{V_{sd0}X_{ts\Sigma}}{V_{s0}X_{q\Sigma}}aV_{c0}\sin(\delta_0 - \gamma_0) + \frac{V_{sq0}X_{ts\Sigma}}{V_{s0}X_{d\Sigma}'}aV_{c0}\cos(\delta_0 - \gamma_0)$$

$$C_3 = -\frac{V_{sd0}X_{ts\Sigma}}{V_{s0}X_{q\Sigma}}aV_{c0}\cos(\delta_0 - \gamma_0) + \frac{V_{sq0}X_{ts\Sigma}}{V_{s0}X_{d\Sigma}'}aV_{c0}\sin(\delta_0 - \gamma_0)$$